Differential inhibition of macrophage foam-cell formation and atherosclerosis in mice by PPARα, β/δ, and γ

Andrew C. Li,[1] Christoph J. Binder,[2] Alejandra Gutierrez,[3] Kathleen K. Brown,[4] Christine R. Plotkin,[5] Jennifer W. Pattison,[2] Annabel F. Valledor,[1] Roger A. Davis,[3] Timothy M. Willson,[6] Joseph L. Witztum,[2] Wulf Palinski,[2] and Christopher K. Glass[1,2]

[1]Department of Cellular and Molecular Medicine and [2]Department of Medicine, University of California, San Diego, La Jolla, California, USA. [3]Department of Biology, San Diego State University, San Diego, California, USA. [4]Department of Metabolic Diseases, GlaxoSmithKline, Research Triangle Park, North Carolina, USA. [5]Genomics Core, Center for AIDS Research, Veterans Medical Research Foundation, La Jolla, California, USA. [6]Department of Medicinal Chemistry, GlaxoSmithKline, Research Triangle Park, North Carolina, USA.

PPARα, β/δ, and γ regulate genes involved in the control of lipid metabolism and inflammation and are expressed in all major cell types of atherosclerotic lesions. In vitro studies have suggested that PPARs exert antiatherogenic effects by inhibiting the expression of proinflammatory genes and enhancing cholesterol efflux via activation of the liver X receptor–ABCA1 (LXR-ABCA1) pathway. To investigate the potential importance of these activities in vivo, we performed a systematic analysis of the effects of PPARα, β, and γ agonists on foam-cell formation and atherosclerosis in male LDL receptor–deficient (LDLR$^{-/-}$) mice. Like the PPARγ agonist, a PPARα-specific agonist strongly inhibited atherosclerosis, whereas a PPARβ-specific agonist failed to inhibit lesion formation. In concert with their effects on atherosclerosis, PPARα and PPARγ agonists, but not the PPARβ agonist, inhibited the formation of macrophage foam cells in the peritoneal cavity. Unexpectedly, PPARα and PPARγ agonists inhibited foam-cell formation in vivo through distinct ABCA1-independent pathways. While inhibition of foam-cell formation by PPARα required LXRs, activation of PPARγ reduced cholesterol esterification, induced expression of ABCG1, and stimulated HDL-dependent cholesterol efflux in an LXR-independent manner. In concert, these findings reveal receptor-specific mechanisms by which PPARs influence macrophage cholesterol homeostasis. In the future, these mechanisms may be exploited pharmacologically to inhibit the development of atherosclerosis.

Introduction

PPARα, PPARβ (also referred to as δ), and PPARγ are members of the nuclear receptor superfamily that regulate gene expression in response to the binding of fatty acids and their metabolites (reviewed in refs. 1–4). PPARs regulate the expression of genes that control lipid metabolism by binding as heterodimers with retinoid X receptors to PPAR response elements in the promoter and/or enhancer regions of these genes (1, 5). PPARs also inhibit expression of proinflammatory genes in a ligand-dependent manner, in part by inhibiting the actions of NF-κB and activator protein 1 (AP-1) family members (6–10). Because of their ability to regulate genes involved in both lipid homeostasis and inflammation, PPARs are promising targets for the development of novel antiatherogenic treatments. In addition to influencing global aspects of lipid and glucose metabolism, PPARs are expressed in the major cell types that make up atherosclerotic lesions, including macrophages, smooth muscle cells, lymphocytes, and endothelial cells, suggest-

ing that ligands for these receptors may act both systemically and locally to influence lesion development (8, 11–15).

In vitro studies indicate that PPARs can exert both atherogenic and antiatherogenic effects on gene expression. Potential atherogenic effects include the ability of PPARα agonists to stimulate the production of monocyte chemoattractant protein 1 (MCP-1) in endothelial cells (16), which would be expected to enhance recruitment of monocytes into lesions (17–19). PPARγ agonists stimulate expression of the scavenger receptor CD36 in macrophages, which facilitates uptake of oxidized LDL (oxLDL) and contributes to the development of atherosclerosis in mouse models (20, 21). Potential antiatherogenic consequences of activating PPARs include the ability of PPARα and PPARγ agonists to inhibit expression of inflammatory response genes — including IFN-γ, IL-1β, IL-6, TNF-α, and C-C chemokine receptor 2 — that promote the recruitment of monocytes and T cells into lesions and their subsequent differentiation and activation (8, 22–25). PPARα and PPARγ have also been demonstrated to stimulate cholesterol efflux in cultured macrophages by inducing the expression of liver X receptor α (LXRα), which in turn activates expression of ABCA1 and other genes involved in cholesterol efflux (26, 27). PPARβ agonists exert variable effects on cholesterol efflux. A PPARβ-specific agonist (GW501516) has been shown to enhance reverse cholesterol transport in a human macrophage cell line (THP-1), in skin fibroblasts (1BR3N), and in intestinal cells (FHS74), and to increase plasma HDL levels in obese, insulin-resistant rhesus monkeys (28). On the other hand, a different PPARβ agonist has

Table 1
Total cholesterol, triglyceride, and HDL levels

	0 Week	4 Weeks	8 Weeks	12 Weeks	14 Weeks
Total cholesterol (md/dl)					
Control ($n = 8$)	285 ± 28	1,486 ± 113	2,011 ± 198	1,950 ± 173	2,502 ± 193
PPARα ligand ($n = 9$)	286 ± 11	1,424 ± 116	2,002 ± 135	2,013 ± 168	2,280 ± 168
PPARβ ligand ($n = 10$)	274 ± 18	1,387 ± 28	2,064 ± 64	2,113 ± 76	2,052 ± 175
Total triglycerides (mg/dl)					
Control	289 ± 28	248 ± 49	338 ± 94	349 ± 39	990 ± 156
PPARα ligand	286 ± 11	221 ± 33	348 ± 78	313 ± 70	634 ± 62
PPARβ ligand	274 ± 18	167 ± 28	317 ± 64	420 ± 76	462 ± 175[A]
HDL (mg/dl)					
Control					189 ± 9
PPARα ligand					201 ± 15
PPARβ ligand					195 ± 7

Data are expressed as mean ± SEM; n represents the number of mice per group. Values were determined in plasma samples from fasting animals. [A]$P < 0.001$.

also been shown to promote lipid accumulation in THP-1 cells and primary human macrophages (29).

Studies of PPARα in mouse models of atherosclerosis have yielded conflicting results. Mice lacking both PPARα and apoE developed less atherosclerosis than mice lacking only apoE when fed a high-fat, high-cholesterol (HC) diet, suggesting a net atherogenic effect of PPARα in this model (30). In contrast, the PPARα agonist fenofibrate exerted minimal antiatherogenic effects in apoE-deficient mice (31, 32), but a more pronounced effect in apoE-deficient mice carrying a fenofibrate-inducible human apoAI transgene (32). Studies of PPARγ-specific agonists in mouse models of atherosclerosis have demonstrated protective effects in male mice that correlate with anti-inflammatory effects in the artery wall and enhanced cholesterol efflux in cultured macrophages (31, 33–35). Furthermore, bone marrow transplantation of LDL receptor–deficient (LDLR$^{-/-}$) mice with wild-type or PPARγ-knockout bone marrow progenitor cells demonstrated an antiatherogenic role of PPARγ in macrophages (26). PPARβ agonists have not been evaluated in models of atherosclerosis, but bone marrow transplantation experiments in which LDLR$^{-/-}$ mice were reconstituted with PPARβ$^{-/-}$ bone marrow progenitor cells suggest that unliganded PPARβ can promote development of atherosclerosis (36).

These previous findings support the concept that PPARs regulate programs of gene expression that influence the development of atherosclerosis, but to our knowledge, the relative importance of proposed protective mechanisms have not been evaluated in vivo. Here, we present a systematic analysis of the effects of specific PPARα and PPARβ agonists on the development of atherosclerosis in male LDLR$^{-/-}$ mice, under conditions similar to those used previously in our laboratory to establish antiatherogenic effects of PPARγ agonists. We examined the effects of specific agonists for all 3 PPAR subtypes on macrophage foam-cell formation and inflammatory gene expression in vivo, and while all 3 PPAR agonists exerted potent anti-inflammatory effects in artery walls of hypercholesterolemic mice containing advanced lesions, only the PPARα and PPARγ agonists inhibited the development of atherosclerosis. Consistent with this, the PPARα and PPARγ agonists, but not the PPARβ agonist, inhibited the formation of macrophage foam cells in vivo. Unexpectedly, the present report of cholesterol uptake and efflux pathways in these cells suggests that

PPARα and PPARγ agonists inhibit foam-cell formation at least in part through distinct ABCA1-independent mechanisms.

Results

Effects of PPARα and PPARβ agonists on atherosclerosis. To investigate potential effects of PPARα and PPARβ on atherosclerosis, we performed intervention studies in LDLR$^{-/-}$ male mice using 2 potent receptor-specific agonists under conditions in which we previously demonstrated that 2 PPARγ agonists, rosiglitazone and GW7845, significantly inhibit lesion development (33). The PPARα-specific agonist GW7647 has a median effective concentration (EC$_{50}$) of 1 nM for the murine PPARα, compared to 2.9 μM and 1.3 μM for murine PPARβ and PPARγ, respectively (37). The PPARβ agonist GW0742 has an EC$_{50}$ of 28 nM for murine PPARβ, versus 8.8 μM and at least 10 μM for murine PPARα and PPARγ, respectively (38). LDLR$^{-/-}$ mice were fed a hypercholesterolemic diet with or without PPAR agonists for 14 weeks. Within 8 weeks, total plasma cholesterol reached approximately 2,000 mg/dl in the control, PPARα agonist–, and PPARβ agonist–treated groups. Total cholesterol levels were not significantly different among the groups and a significant reduction in the triglyceride levels in mice treated with the PPARβ agonist was only noted at the final time point (Table 1). HDL levels remained unchanged. No adverse health effects were noted throughout the study. Animals treated with the PPARα agonist had a significantly higher ($P < 0.001$) liver to body weight ratio (0.079 ± 0.004, mean ± SEM) compared to animals treated with the PPARβ agonist (0.057 ± 0.002) or to control animals (0.049 ± 0.004).

The extent of atherosclerosis was determined in en face preparations of the entire aorta after 14 weeks of the HC diet (Figure 1, A and B). Treatment with the PPARα agonist yielded a 50% reduction in atherosclerosis in the aortic arch and nearly a 90% reduction in both the descending thoracic aorta (DTA) and abdominal aorta. In contrast, the extent of atherosclerosis in animals receiving the PPARβ agonist was not significantly different from that of control animals in the arch or in the DTA. Atherosclerosis was also assessed in cross-sections through the aortic origin (Figure 1, C and D). Consistent with the results throughout the aorta, animals that were fed the PPARα agonist exhibited an approximately 50% reduction in cross-sectional lesion area compared to the control group. This effect was similar to the 40–70% reduction in lesion area previously observed for PPARγ agonists under similar experimental conditions (33). Again, lesion size in animals fed the PPARβ agonist was not significantly different from that of controls.

Metabolic effects of PPARα and PPARβ agonists. To investigate whether metabolic differences might have contributed to the difference in antiatherogenic effect of the 2 agonists, we compared weight, insulin levels, and lipoprotein profiles (Figure 2). Animals fed the PPARα agonist gained less weight compared with controls or animals fed the PPARβ agonist (Figure 2A), and they exhibited less adipose tissue. All animals consumed similar amounts of food throughout the study. Insulin levels were also significantly lower in animals treated with the PPARα agonist (Figure 2B). Fast-performance liquid chromatography (FPLC) analysis revealed a modest relative reduction
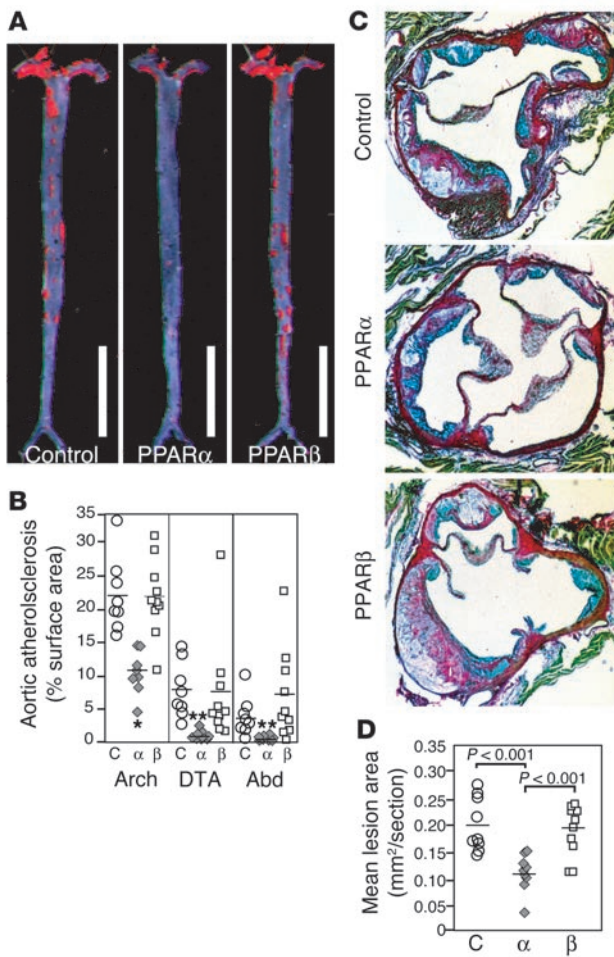
Figure 1
Atherosclerosis in LDLR$^{-/-}$ male mice that were fed the HC diet for 14 weeks. (**A**) Sudan IV–stained en face preparations of aortas. Scale bars: 1 cm. (**B**) Quantitative analysis of atherosclerotic surface area in the entire aorta. (**C**) Sections through the aortic root at the level of the aortic valves. The micrographs are taken of sections at a similar distance from the aortic root. Original magnification, ×4. (**D**) Quantitative analysis of lesion areas in the aortic root. Data expressed as the mean ± SEM. C, control; α, PPARα agonist GW7647; β, PPARβ agonist GW0742; Abd, abdominal aorta; Arch, aortic arch. *$P < 0.001$ and **$P \leq 0.02$, compared with control.

actually upregulated in early lesions by the PPARα-specific agonist (data not shown), consistent with a previous report (16). Overall, however, these differences did not correlate with the effects of each PPAR agonist on the extent of atherosclerosis.

Influence of PPARα, β, and γ agonists on genes regulating macrophage cholesterol metabolism in vivo. To investigate the effects of PPAR agonists on genes directly involved in foam-cell formation and cholesterol efflux in the artery wall, we used real-time PCR to measure mRNA levels of macrosialin, CD36, ABCA1, and LXRα in established atherosclerotic lesions (Figure 3). Aortas isolated from hypercholesterolemic mice exhibited a marked increase in macrosialin expression, consistent with an increased presence of intimal macrophages. As seen previously, increased macrosialin expression was not accompanied by a concomitant increase in CD36 expression (33). Further increase of CD36 expression was observed only with the PPARγ agonist. Expression of ABCA1 also increased in hypercholesterolemic mice and was associated with the increased expression of LXRα. However, none of the PPAR agonists altered the expression of ABCA1, even though the expression of LXRα was increased in mice treated with the PPARα agonist. Although it is possible that ABCA1 is upregulated by PPAR ligands in a subset of cells within the aorta, these results suggest that upregulation of ABCA1 mRNA expression in the arterial wall is not the mechanism by which PPARα and γ agonists inhibit the development of atherosclerosis.
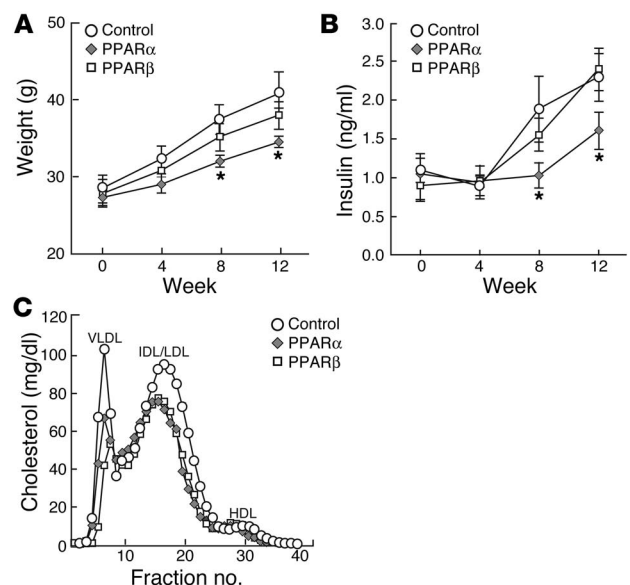
Influence of PPAR agonists on scavenger receptor activity in primary macrophages. To determine whether the effect of PPAR agonists on
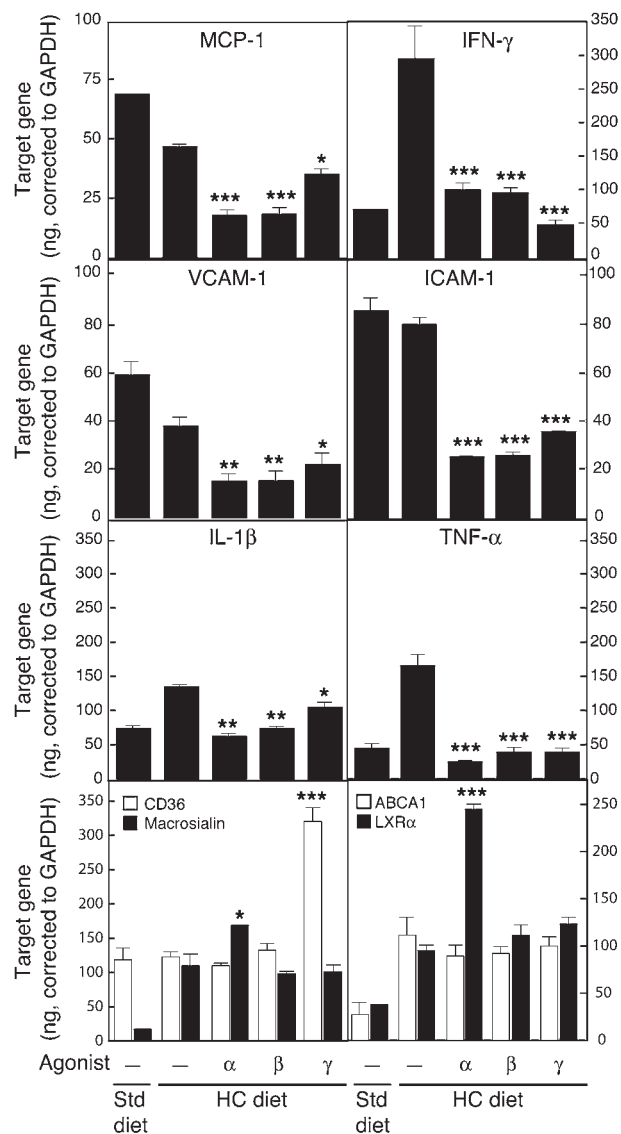
in the VLDL, IDL/LDL, and HDL fractions in both of the treated groups, compared to the control group (Figure 2C).

Effects of PPARα, β, and γ agonists on inflammatory gene expression. To examine the effects of PPAR agonists within the artery wall, we analyzed gene expression in animals with extensive atherosclerosis that were fed either the HC diet alone or the HC diet plus agonists for 14 weeks. All 3 PPAR agonists significantly inhibited the expression of IFN-γ, TNF-α, MCP-1, VCAM-1, and ICAM-1, whereas lesser effects were observed for IL-1β (Figure 3). Experiments were also performed in younger mice with earlier lesions. These studies indicated some differences in the expression patterns of inflammatory markers and their responses to drug treatment. For example, IFN-γ was not detected in earlier lesions, consistent with low absolute numbers of lymphocytes at this time point. MCP-1 levels, which were downregulated by all 3 PPAR agonists in late lesions, were

Figure 2
Metabolic effects of PPAR ligands. Weight (**A**), plasma insulin levels (**B**), and size distribution (**C**) of lipoprotein particles fractionated by FPLC. Measurements of weight and plasma insulin levels were taken at the indicated time points. FPLC analysis of lipoproteins was done using pooled plasma from terminal bleeds. Circles, control; diamonds, PPARα agonist GW7647; squares, PPARβ agonist GW0742. Data are expressed as mean ± SEM. *$P \leq 0.05$ compared with control. Measurements are from individual animals shown in Figure 1. Control, $n = 8$; PPARα agonist, $n = 9$; PPARβ agonist, $n = 10$.

Figure 3
Gene expression in atherosclerotic lesions determined by real-time PCR analysis. Animals were fed an HC diet for 3 months (resulting in advanced lesions), followed by 4 weeks on the same diet supplemented with the indicated PPAR agonists. Data are expressed as the mean ± SEM of triplicate measurements and are representative of 2 independent experiments. In each case, *$P \leq 0.05$, **$P \leq 0.01$, and ***$P \leq 0.001$, compared with HC. Std, standard.

extent as did the LXR agonist 24 (S), -25-epoxycholesterol (Figure 4C). Consistent with these findings, the PPARγ agonist, but not the PPARα or β agonists, stimulated expression of LXRα RNA (Figure 4D) and ABCA1 RNA and protein levels (Figure 4, E and F) in cholesterol-loaded macrophages.

Influence of PPAR agonists on macrophage foam-cell formation in vivo. Although the ability of rosiglitazone to induce LXRα and ABCA1 expression in cultured macrophages is consistent with previous reports (27, 39), these responses were discrepant with the lack of an effect on the expression of LXRα and ABCA1 in the artery wall (Figure 3). We therefore developed an in vivo model for foam-cell formation by eliciting peritoneal macrophages in LDLR$^{-/-}$ mice that were fed an HC diet. In contrast to macrophages isolated from mice that were fed a normal chow diet, macrophages isolated from hypercholesterolemic mice exhibited extensive Oil red O droplets (Figure 5A). Quantitative lipid analysis indicated a dramatic increase in cholesteryl ester levels, accounting for the major change in neutral lipid content, as well as a modest increase in triglyceride content (Figure 5B). Treatment of animals with the PPARα and PPARγ agonists largely prevented lipid accumulation in these cells. In contrast, treatment with the PPARβ agonist did not reduce total cholesterol accumulation or overall oil red O staining, even though it decreased triglyceride levels and free cholesterol (Figure 5, A and B).

These results were of particular interest because the effects of the 3 PPAR agonists on foam-cell formation within the peritoneal cavity paralleled their effects on the development of atherosclerotic lesions. All 3 PPAR subtypes were found to be expressed in peritoneal macrophages, although PPARα expression was significantly lower than that of PPARβ or PPARγ (Figure 5C). As in the case of primary macrophages treated with PPAR-specific agonists in vitro, CD36 expression was selectively increased in response to the PPARγ agonist (Figure 5D). In contrast to results obtained in cultured macrophages, but consistent with findings in the artery wall, none of the PPAR agonists influenced the expression of ABCA1 or LXRα in foam cells derived from the peritoneal cavity of hypercholesterolemic mice (Figure 5E). These observations suggest that PPAR agonists can inhibit foam-cell formation in vivo by LXR/ABCA1-independent mechanisms.

PPARα agonists require macrophage expression of PPARα to inhibit foam-cell formation. To determine the roles of specific genes in PPAR-dependent inhibition of foam-cell formation, we developed and validated an assay based on the transfer of macrophages from donor animals into LDLR$^{-/-}$ mice. In preliminary experiments, elicited macrophages from wild-type donor animals were injected into the peritoneal cavities of LDLR$^{-/-}$ mice. Three days following injection of 30 million donor cells, 10–15 million cells could be recovered from the peritoneal cavity of the recipient mouse. To determine the fraction of donor cells recovered, donor macrophages bearing 20 copies of the λgt11-*LacZ* transgene (40) were injected

foam-cell formation could be attributed to modulation of scavenger-receptor activity, we measured uptake and degradation of oxLDL in isolated peritoneal macrophages treated in vitro with PPAR agonists for 24 hours (Figure 4A). As previously shown, the PPARγ agonist significantly increased both uptake and degradation of oxLDL (20, 33), whereas treatment with the PPARα agonist did not have a significant effect. The PPARβ agonist had a small but significant effect on the degradation of oxLDL. Effects of PPAR-specific agonists on oxLDL uptake and degradation were closely correlated with their effects on CD36 expression (Figure 4B). Scavenger receptor A (SRA) expression remained unchanged (Figure 4B). These findings suggest that the PPAR agonists do not inhibit foam-cell formation by downregulating scavenger receptors that mediate uptake of pathogenic lipoproteins.

Influence of PPAR agonists on cholesterol efflux pathways in cultured macrophages. Initial experiments were performed to evaluate effects of PPAR agonists on cholesterol efflux and expression of LXRα and ABCA1 in isolated peritoneal macrophages (Figure 4, C–F). The PPARγ agonist, but not the PPARα or β agonists, stimulated apoAI-dependent cholesterol efflux to approximately the same

into recipient mice. This transgene is not normally expressed in mouse macrophages, and the gene itself therefore provides a specific and quantitative marker of the transferred cells. Quantification of the *lacZ* marker indicated that approximately 70% of the peritoneal macrophages that were recovered from recipient mice 3 days following transfer were of donor origin (data not shown).

Macrophages transferred from wild-type donors developed lipid droplets and increased cholesterol and triglyceride content when injected into LDLR$^{-/-}$ mice fed an HC diet (Figure 6, A and B), but not when injected into LDLR$^{-/-}$ recipients fed a normal diet (data not shown). The low levels of PPARα mRNA in peritoneal macrophages (Figure 5C) raised the question of whether the inhibitory effects of PPARα-specific agonists on foam-cell formation in vivo were intrinsic to the macrophage. To address this question, we transferred elicited macrophages from PPARα$^{+/+}$ mice (both C57BL6/J and 129S backgrounds) and PPARα$^{-/-}$ mice (129S background) into hypercholesterolemic LDLR$^{-/-}$ mice treated with or without the PPARα agonist for 4 weeks. The PPARα agonist inhibited foam-cell formation and dramatically reduced cholesteryl ester levels in macrophages derived from wild-type C57BL6 and 129S mice, but not in those from PPARα$^{-/-}$ 129S mice (Figure 6, A and B). These results indicate that the inhibitory effects of the PPARα agonist are both PPARα dependent and intrinsic to the macrophage. These data provide further support for the validity of the peritoneal cell transfer method, since the observed lack of effect of the PPARα-specific agonist in recipient animals receiving PPARα$^{-/-}$ macrophages would not be expected if the majority of peritoneal cells were wild type (Figure 6). Expression of ABCA1 in adoptively transferred PPARα$^{+/+}$ and PPAR$^{-/-}$ macrophages was not altered by treatment with the PPARα agonist, consistent with PPARα regulating cholesterol homeostasis independently of ABCA1 (Figure 6C).

PPARα agonists, but not PPARγ agonists, require LXR to reduce foam-cell formation in peritoneal macrophages. To determine whether PPARα and PPARγ agonists can regulate foam-cell formation through an LXR-independent pathway, we performed macrophage transfer experiments using wild-type and LXR double knockout (DKO) mice. Following transfer into hypercholesterolemic LDLR$^{-/-}$ mice, LXR DKO macrophages stained more intensively with Oil red O and accumulated significantly more cholesteryl esters than did wild-type macrophages (Figure 7, A and B). These results are consistent with LXRs playing an important role in maintenance of cholesterol homeostasis. Triglyceride levels in the LXR DKO macrophages were also much lower, compared to untreated control macrophages, consistent with previous results demonstrating that LXRs play a role in triglyceride metabolism through SREBP-1 (41). As expected, ABCA1 protein levels were reduced in macrophages derived from hypercholesterolemic LXR DKO animals, compared to levels in macrophages derived from hypercholesterolemic wild-type animals (Figure 7C). However, treatment of recipient animals with the PPARγ agonist led to significant reductions in oil red O staining and cholesterol content in both wild-type and LXR DKO macrophages (Figure 7, A and B). Similar results were observed using LXRα$^{-/-}$ macrophages (data not shown). Unexpectedly, when we transferred LXR DKO macrophages into LDLR$^{-/-}$ mice treated with the PPARα agonist, we were unable to recover sufficient LXR DKO macrophages for subsequent analysis (data not shown), raising the possibility that activation of PPARα exerted toxic effects in the absence of LXRs.

To further investigate the role of LXRs in mediating inhibitory effects of PPARα on foam-cell formation using an independent approach, we performed bone marrow transplantation experi-

ments in which bone marrow from either wild-type or LXR DKO mice was used to reconstitute irradiated LDLR$^{-/-}$ mice. Reconstituted mice were fed the HC diet and treated with PPARα or PPARγ agonists or control solvent prior to elicitation of peritoneal macrophages for analysis of foam-cell formation. Real-time PCR confirmed the absence of both LXRα and β in these macrophages (Figure 7D). Treatment with the PPARγ agonist rosiglitazone significantly inhibited foam-cell formation, consistent with results of the peritoneal macrophage transfer experiments. In contrast, treatment with the PPARα agonist dramatically reduced the number of viable LXR DKO macrophages that could be isolated from the peritoneal cavity, also consistent with the results of peritoneal macrophage transfer experiments. The few cells that were obtained
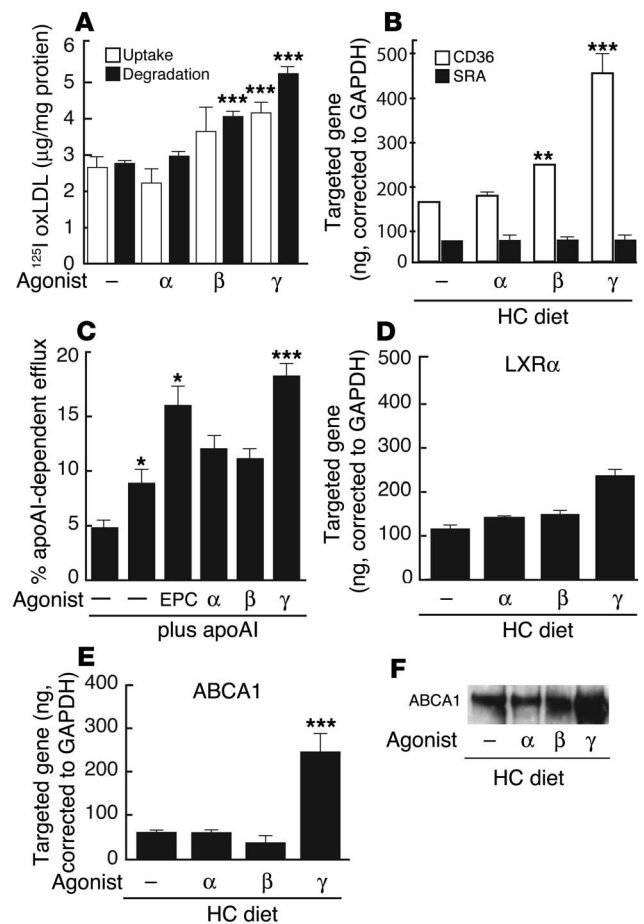
Figure 4
Determination of scavenger receptor activity and cholesterol efflux in cultured peritoneal macrophages. PPAR-specific agonists, as indicated. (**A**) Influence of PPAR agonists on uptake (white bars) and degradation (black bars) of oxLDL. (**B**) Influence of PPAR agonists on CD36 and SRA expression by real-time PCR in hypercholesterolemic macrophages. (**C**) Influence of LXR and PPAR agonists on apoAI and HDL-specific cholesterol efflux in acLDL-loaded peritoneal macrophages. Expression of LXRα (**D**) and ABCA1 (**E**) by real-time PCR in hypercholesterolemic macrophages treated with PPAR agonists in vitro. (**F**) Western blot analysis of ABCA1 protein in hypercholesterolemic macrophages treated with PPAR agonists as in **E**. Data are mean ± SEM and are representative of at least 2 independent experiments. In each case, *$P \leq 0.05$, **$P \leq 0.01$, and ***$P < 0.001$ compared with control. EPC, 24 (S), -25-epoxycholesterol; ^{125}I oxLDL, ^{125}I-labeled oxLDL.
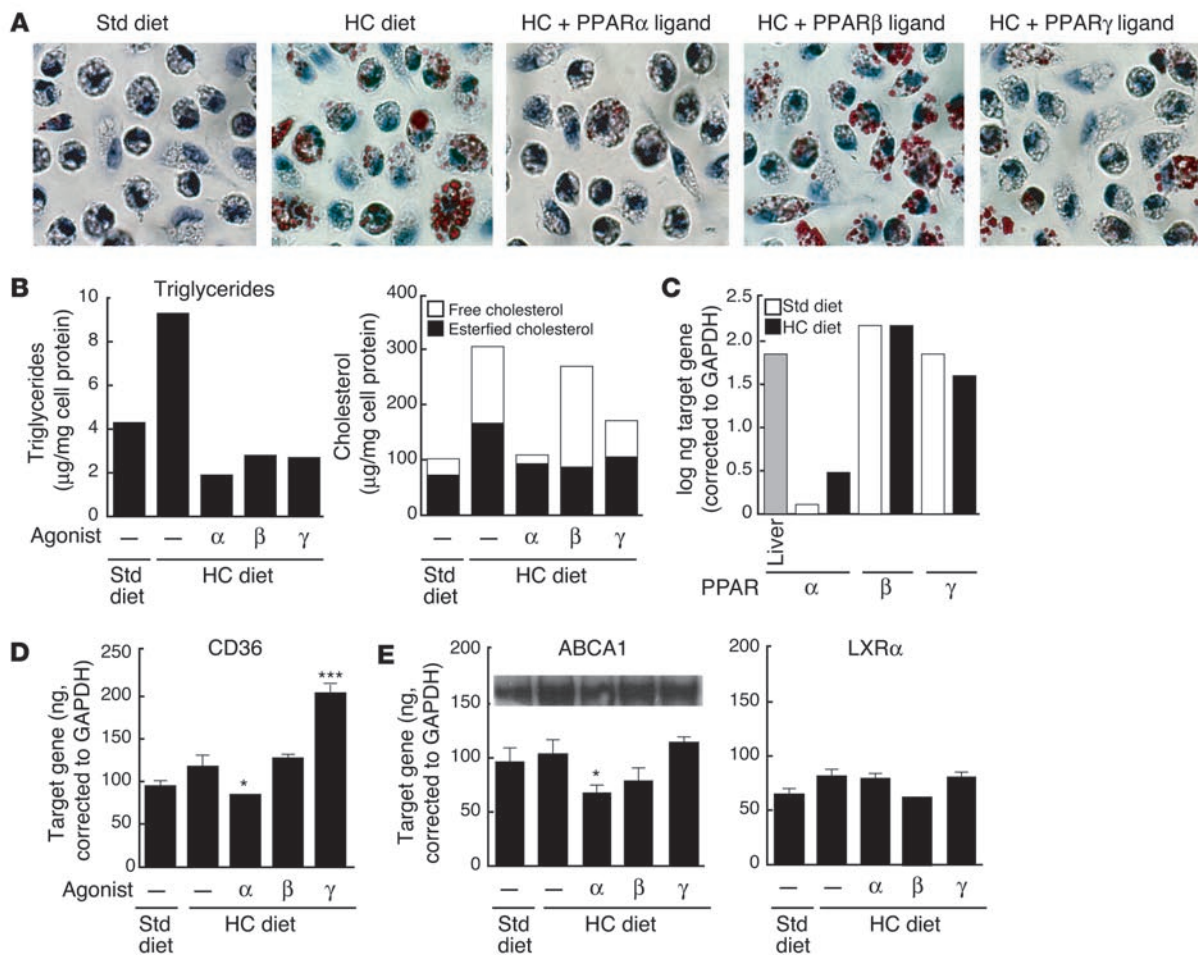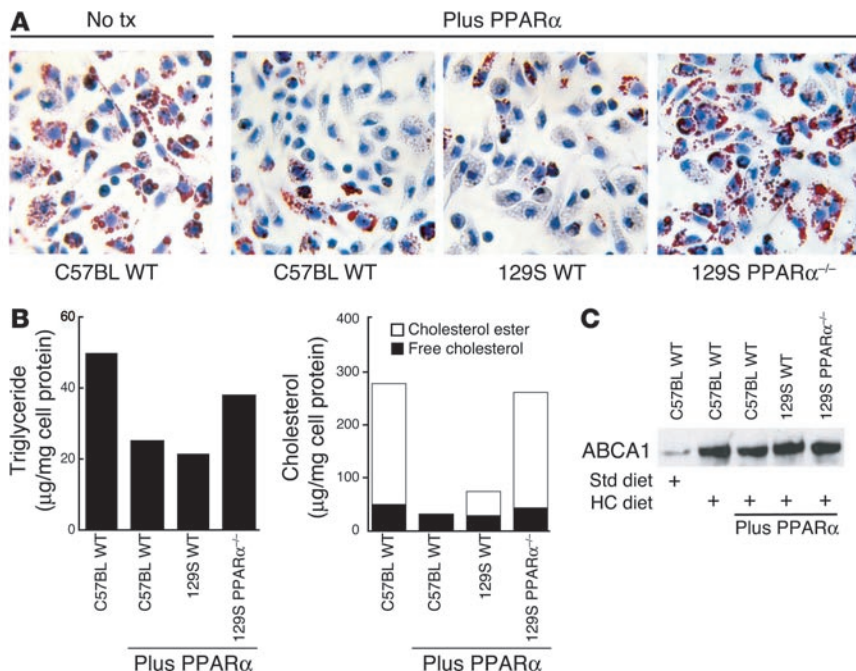
Figure 5

Effects of PPAR-specific ligands on macrophage foam-cell formation in vivo. LDLR$^{-/-}$ mice were fed a control or HC diet for 4 months and were treated for the last month with PPAR-specific agonists, as indicated. Mice were injected intraperitoneally with thioglycollate after the fourth week of drug treatment and peritoneal macrophages were harvested 4 days later for analysis. (**A**) Oil red O staining. Original magnification, ×40. (**B**) Quantification of triglycerides and cholesterol. For cholesterol values, total bar height represents total cholesterol. The free cholesterol component is represented by a black bar and esterified cholesterol, calculated as total cholesterol minus free cholesterol, is represented by a white bar. Data are expressed as micrograms per milligram of cell protein and are representative of 2 independent experiments. (**C**) Expression of PPARα, β, and γ in normal (white bars) and hypercholesterolemic (black bars) macrophages. Liver is included as a positive control for a tissue expressing relatively high levels of PPARα. (**D**) Expression of CD36 mRNA levels determined by real-time PCR. (**E**) Expression of ABCA1 and LXRα mRNA levels determined by real-time PCR and Western analysis. Real-time PCR data expressed are mean ± SEM. The results are representative of 2 independent experiments. *$P \leq 0.05$ versus control, ***$P < 0.001$ versus HC control.

were massively engorged with lipid droplets that almost completely filled the cytoplasmic compartment (Figure 7E). Although it was not possible to isolate sufficient cells for reliable measurement of cholesterol ester levels, these experiments indicate that in contrast to PPARγ agonists, the ability of PPARα agonists to inhibit foam-cell formation requires LXRs. The basis for low recovery of LXR DKO macrophages in mice treated with the PPARα agonist remains to be established. PPARα and PPARγ have been reported to differentially induce apoptosis in human monocyte–derived macrophages (42), raising the possibility that activation of PPARα results in a strong proapoptotic effect in the absence of LXRs.

Influence of PPAR agonists on cholesterol esterification. To investigate potential roles of PPARs in regulation of cholesterol esterification, we loaded peritoneal macrophages with cholesterol by incubation with aggregated LDL (agLDL), followed by the addition of a mixture

of C^{14} radiolabeled and unlabeled oleic acid (43). As expected, the addition of agLDL increased the cholesterol esterification rate from less than 1% (in the unloaded cells) to 25% (Figure 8A). Addition of an Acyl-CoA: cholesterol acyltransferase (ACAT) inhibitor effectively reduced esterification in cells incubated with agLDL to less than 2%. In cells treated with either the PPARα or PPARβ agonist, the rate of esterification did not significantly change. However, rosiglitazone reduced esterification by more than 50% (Figure 8A). This effect was independent of the LXR pathway because similar results were obtained when the esterification assay was performed in LXR DKO peritoneal macrophages (Figure 8A). Rosiglitazone treatment did not significantly alter the mRNA levels of ACAT1 (Figure 8B) or neutral cholesterol ester hydrolases (data not shown).

PPARγ regulates ABCG1 expression. Recent studies have identified ABCG1 as an LXR target gene that mediates transfer of choles-

Figure 6
Effects of the PPARα agonist on foam-cell formation are intrinsic to the macrophage. Transfer of thioglycollate-elicited PPARα wild-type and PPARα⁻/⁻ peritoneal macrophages. Elicited macrophages were isolated from wild-type C57BL/6J (C57BL WT), 129SU/SvImJ (129S WT), or PPARα⁻/⁻ 129SU/SvImJ (129S PPARα⁻/⁻) mice. We injected 3 × 10⁷ cells of each genotype into the peritoneal cavities of hypercholesterolemic LDLR⁻/⁻ mice. Cells were recovered from the peritoneal cavity for analysis by Oil red O staining (**A**). No tx, no treatment. Original magnification, ×40. (**B**) Measurement of triglyceride and cholesterol content as in Figure 5. (**C**) Western blotting of ABCA1 protein. The results are representative of at least 2 independent experiments.

terol to HDL acceptors (44–46). To investigate whether ABCG1 might also be a target of a PPARγ-dependent, LXR-independent pathway, real-time PCR experiments were performed in peritoneal macrophages isolated from wild-type and LXR DKO mice. These studies demonstrated that the PPARγ agonist, but not the PPARα or PPARβ agonists, induced ABCG1 expression in both wild-type and LXR DKO macrophages (Figure 8, C and E). No effects on ABCA1 expression were observed, consistent with previous results (Figure 8D). Furthermore, treatment of hypercholesterolemic LDLR⁻/⁻ mice with the PPARγ agonist significantly increased expression of ABCG1 in aortas containing extensive atherosclerotic lesions (Figure 8F). Finally, activation of PPARγ significantly enhanced HDL-dependent cholesterol efflux from LXR DKO macrophages (Figure 8G).

Discussion

Differential inhibition of atherosclerosis by PPAR subtypes. Studies from our laboratory and others have documented that PPARγ ligands inhibit the development of atherosclerosis in mouse models (31, 33–35). Here, we demonstrate that a PPARα agonist but not a PPARβ agonist, inhibits the development of atherosclerosis in male LDLR⁻/⁻ mice under very similar experimental conditions. Cholesterol and triglyceride levels were not sufficiently different between PPARα and PPARβ agonist treatment groups to account for the different effects on lesion development. PPARα-treated mice exhibited improved insulin sensitivity and reduced weight gain, which may have contributed in part to the antiatherosclerotic effects. Reduced weight gain in PPARα-treated animals is consistent with previous findings (47). Although the PPARβ agonist did not inhibit the development of atherosclerosis in this model, there appear to be significant species-specific differences in the action of PPARβ agonists. For example, a PPARβ agonist has been shown to raise HDL levels, reduce triglycerides, and improve insulin sensitivity in obese monkeys (28).

The observation that activation of PPARα results in net antiatherogenic effects in LDLR⁻/⁻ mice is in apparent conflict with studies

in PPARα⁻/⁻ apoE⁻/⁻ mice, in which the lack of PPARα was associated with decreased atherosclerosis (30). However, the generation of a null allele for a nuclear receptor does not always result in a phenotype opposite that induced by administration of a receptor agonist. This discrepancy is clearly illustrated by the observation that deletion of the PPARα gene in the context of the apoE⁻/⁻ background resulted in increased insulin sensitivity in the setting of a high-fat diet (30), while in the present studies administration of the PPARα agonist also increased insulin sensitivity. The results from the present study are also quantitatively different from the results of studies using fenofibrate in apoE⁻/⁻ mice. Duez et al. (32) demonstrated that treatment of apoE-deficient mice with fenofibrate did not reduce lesion size at the aortic origin, but did reduce cholesterol content along the descending aorta in older mice. Significant reduction in lesion size was only observed when fenofibrate was given to apoE-deficient mice possessing a human apoAI transgene, which is responsive to PPARα ligands and leads to increased HDL levels (48). The apparent discrepancies between the present studies and those of Duez et al. (32) and Tordjman et al. (30) could be explained if apoE plays a role in mediating antiatherogenic effects of PPARα, for example by acting as a cholesterol acceptor in an ABCA1-independent efflux pathway. In addition, the PPARα-specific agonist used in these studies (GW7647) has a much higher affinity for PPARα than does fenofibrate and may have been more effective at activating PPARα in peripheral tissues.

Anti-inflammatory actions of PPAR-specific agonists. The importance of inflammatory mechanisms in modulating the development of atherosclerosis has been clearly demonstrated by analysis of compound knockout and transgenic mouse models that carry alleles conferring gain or loss of function of critical inflammatory regulators in the setting of diet-induced hypercholesterolemia (reviewed in refs. 4, 49–51). We observed that the PPARα-, PPARβ-, and PPARγ-specific agonists used in these studies strongly inhibited the expression of several genes associated with the development of atherosclerosis, including VCAM-1, MCP-1, and IFN-γ (Fig-
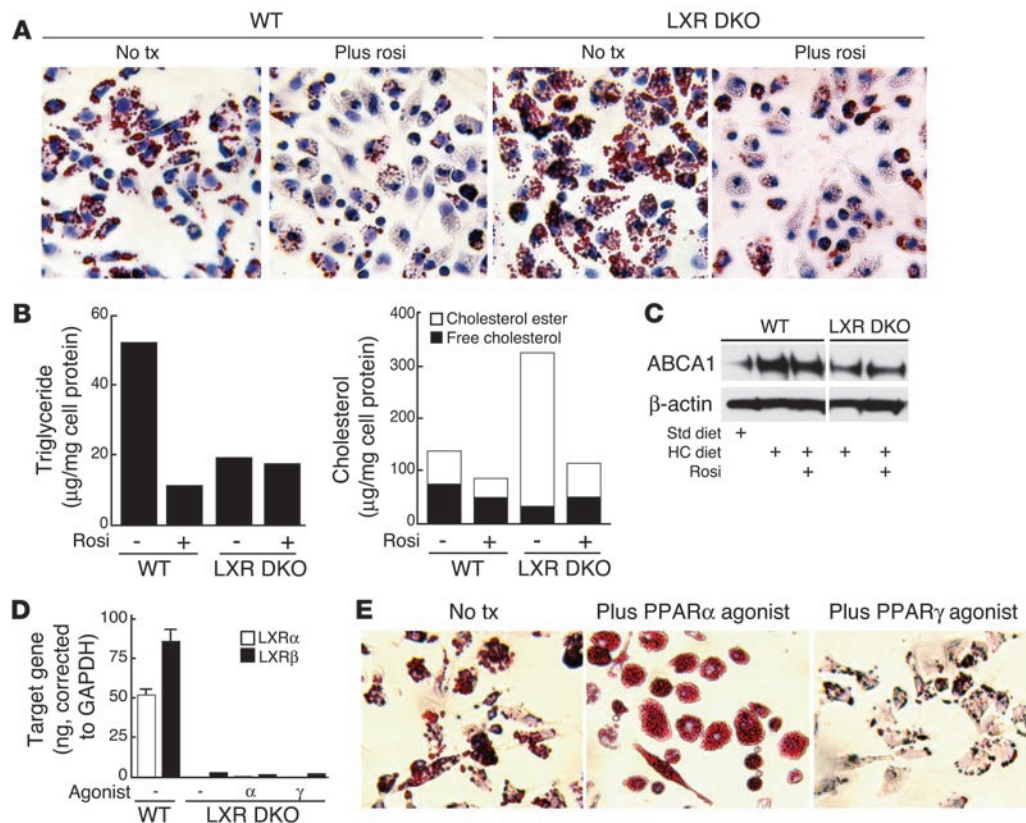
Figure 7

PPARα, but not PPARγ, agonists require LXR to reduce foam-cell formation in peritoneal macrophages. (**A**) Transfer of thioglycollate-elicited wild-type and LXR DKO peritoneal macrophages into hypercholesterolemic LDLR⁻/⁻ mice treated with rosiglitazone (rosi) or control solvent (No tx) for 4 weeks. Macrophages were stained with Oil red O. Original magnification, ×40. (**B**) Quantification of triglycerides and cholesterol in transferred macrophages as described in Figure 5. (**C**) Western blot analysis of ABCA1 protein levels in transferred peritoneal macrophages. (**D**) Real-time PCR analysis of LXRα and LXRβ expression in peritoneal macrophages derived from irradiated LDL-R⁻/⁻ mice reconstituted with bone marrow derived from either wild-type or LXR DKO mice. (**E**) Oil red O staining of peritoneal macrophages isolated from hypercholesterolemic LDLR⁻/⁻ mice reconstituted with LXR DKO bone marrow under the following treatment conditions: no treatment, PPARα agonist, or PPARγ agonist. Original magnification, ×40.

ure 3). Lee et al. (36) recently reported that hypercholesterolemic LDLR⁻/⁻ mice reconstituted with PPARβ⁻/⁻ bone marrow cells develop less atherosclerosis than do mice reconstituted with wild-type cells. Analysis of the PPARβ⁻/⁻ phenotype indicated that the unliganded form of PPARβ interacts strongly with B cell leukemia/lymphoma 6 (Bcl6), a repressor protein that negatively regulates the expression of MCP-1. Lee et al. (36) proposed that in PPARβ⁻/⁻ macrophages, Bcl6 is free to bind to the MCP-1 promoter, inhibiting its expression and thereby reducing atherosclerosis. In wild-type macrophages, a PPARβ-specific agonist displaced Bcl6 from PPARβ, also resulting in inhibition of MCP-1 expression. In the present studies, a PPARβ-specific agonist inhibited a broad spectrum of inflammatory gene expression to approximately the same extent as the PPARα and PPARγ agonists did, suggesting that PPARβ can inhibit inflammatory gene expression through additional mechanisms. Although this was not sufficient to result in a net antiatherogenic effect in this model, the extreme levels of hypercholesterolemia achieved in these studies may have reduced the impact of anti-inflammatory effects on lesion development. Studies of mice deficient in *recombinase activating gene 1* (*Rag-1*) crossed with apoE⁻/⁻ (52) or LDLR⁻/⁻ mice (53) have suggested that the influence of immune mechanisms in atherogenesis is more

pronounced at more moderate levels of hypercholesterolemia. It will, therefore, be important to determine whether PPARβ-specific agonists exert antiatherogenic effects under conditions of mild hypercholesterolemia that are more typical of human disease.

PPARs, LXRs, and foam-cell formation. Gene deletion studies and the use of synthetic LXR agonists indicate that LXRs have important antiatherogenic effects in mouse models, and that these effects are correlated with enhanced apoAI-dependent cholesterol efflux from macrophages (54, 55). PPARα and PPARγ ligands have been suggested to influence cholesterol homeostasis in the macrophage by inducing the expression of LXRα (26, 27). In the present studies, we found that the ability of PPAR-specific agonists to regulate LXR and ABCA1 expression is context dependent. Within the artery wall, LXRα expression was induced by the PPARα-specific agonist. This result was observed both in the normal vessel wall (data not shown) and in arteries with extensive atherosclerotic lesions (Figure 3) and may reflect effects on cells other than macrophages. In macrophages loaded in vitro with cholesterol through exposure to acetylated LDL (acLDL), the PPARγ-specific agonist induced LXRα and ABCA1 expression (Figure 4). In contrast, none of the PPAR-specific agonists altered ABCA1 expression in arteries with extensive atherosclerosis (Figure 3). Furthermore, none of the PPAR agonists
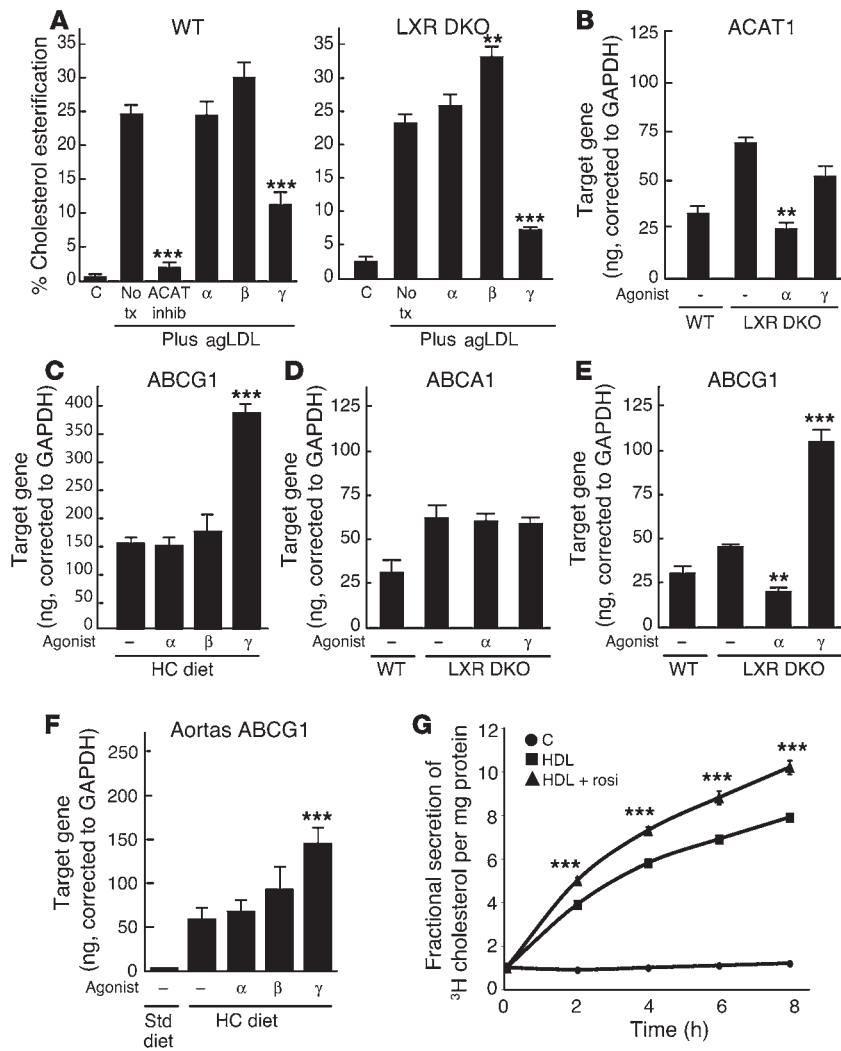
Figure 8
PPARγ inhibits cholesterol esterification and stimulates ABCG1 expression in an LXR-independent manner. (**A**) The PPARγ agonist rosiglitazone inhibited cholesterol esterification in both wild-type and LXR DKO macrophages subjected to cholesterol loading with agLDL. The results are representative of at least 2 independent experiments. (**B**) Real-time PCR analysis of ACAT1 mRNA expression in wild-type and LXR DKO macrophages. (**C**) Rosiglitazone induced ABCG1 expression in macrophages isolated from hypercholesterolemic LDLR$^{-/-}$ mice. Rosiglitazone had no effect on ABCA1 expression (**D**) but induced ABCG1 expression in LXR DKO macrophages isolated from LDLR$^{-/-}$ mice (**E**). (**F**) Rosiglitazone induced ABCG1 expression in aortas of hypercholesterolemic LDLR$^{-/-}$ mice containing extensive lesions. (**G**) Rosiglitazone induced HDL-specific cholesterol efflux in macrophages. Data are expressed as mean ± SEM. **$P \leq 0.01$ and ***$P < 0.001$, compared with the no-treatment control.

of foam-cell formation. Using this approach, the effects of PPARα agonists on macrophage foam-cell formation were demonstrated to be intrinsic to the macrophage, despite relatively low levels of PPARα mRNA.

Macrophage transfer and bone marrow reconstitution experiments also indicated that the ability of PPARα to inhibit foam-cell formation required LXRs, but did not correlate with effects on ABCA1 expression. The LXR-dependent genes required for the actions of PPARα are not clear, but could potentially include apoE. The expression of apoE was not altered by PPAR agonists in these studies (data not shown), despite the presence of a potential PPAR response element in the apoE promoter (56). A critical role of apoE as an LXR target gene could at least partially reconcile the lack of a strong inhibitory effect of PPARα agonists on development of atherosclerosis in apoE$^{-/-}$ mice (30, 32).

In contrast, the ability of PPARγ to inhibit foam-cell formation was clearly independent of both LXRs and ABCA1. Investigation of alternative pathways regulating cholesterol homeostasis revealed 2 additional PPARγ-sensitive targets. First, rosiglitazone inhibited cholesterol esterification in an LXR-independent manner. This effect was not due to downregulation of ACAT1 mRNA expression; it may have resulted from indirect effects on transfer of cholesterol for esterification or posttranslational effects on ACAT1 activity. Although not observed in these studies, activation of PPARα was previously shown to inhibit cholesterol esterification in human macrophages without affecting ACAT1 gene expression (57). The basis for different effects of PPARα agonists in human and mouse macrophages is not clear, but it may relate to relatively higher levels of PPARα in human monocytes and/or macrophages. Although studies have shown that ACAT1 deficiency worsens atherosclerosis (58, 59), there is also evidence that partial inhibition of ACAT1 activity by drugs reduces the development of atherosclerosis (60).

induced LXRα or ABCA1 expression in peritoneal macrophages isolated from hypercholesterolemic LDLR$^{-/-}$ mice (Figure 5), yet the PPARα- and PPARγ-selective agonists strongly inhibited foam-cell formation in this setting. One possible explanation for the discrepancy between in vitro and in vivo results is that the expression of ABCA1 is already maximally expressed in the setting of extreme hyperlipidemia, precluding any further effect of PPARγ agonists. Consistent with this, ABCA1 expression was upregulated in the artery wall in response to rosiglitazone at early time points of HC feeding (data not shown), suggesting that it may contribute to antiatherogenic effects of PPARγ agonists. Experiments evaluating the efficacy of PPARγ agonists in the background of ABCA1 deficiency will be required to resolve this issue.

Identification of PPAR-dependent and LXR-independent pathways that regulate macrophage foam-cell formation. To define the requirements for effects of PPAR agonists on foam-cell formation in vivo, we evaluated the ability of macrophages derived from donor mice of varying genotypes to accumulate cholesterol following transfer into the peritoneal cavities of hypercholesterolemic mice. This approach was validated by several methods, including comparison with bone marrow reconstitution experiments. Transfer of peritoneal macrophages thus appears to provide a useful method for rapidly determining the roles of specific genes in the regulation

Table 2
Summary of the effects of the PPAR-selective ligands on atherosclerosis

Effect on	PPARα	PPARβ/δ	PPARγ
Atherosclerosis	↓	−	↑[A]
Body weight	↓	−	−[A]
Insulin levels	↓	−	↑[A]
Cholesterol levels	−	−	−
CD36 expression	−	↑	↑↑
Inflammation	↓	↓	↓
Foam-cell formation	↓[B]	−[B]	↓[B]
ABCA1 expression	−[B]	−[B]	−[B]
ABCG1 expression	−[B]	−[B]	↑↑
Cholesterol esterification	−	−	↓

[A]Data from Li et al. (33). [B]Measured in macrophage foam cells derived from hypercholesterolemic mice. ↑, upregulated; ↑↑, highly upregulated; ↓, downregulated.

In addition, the present studies demonstrate that PPARγ agonists induce expression of ABCG1 in primary macrophages and in the artery walls of hypercholesterolemic mice. We previously identified ABCG1 as a PPARγ target gene using conditional PPARγ-deficient macrophages (61). Here, we demonstrate that induction of ABCG1 also occurs in LXR DKO macrophages, thereby establishing ABCG1 as an LXR-independent target of PPARγ. Recent studies demonstrate that ABCG1 is also a target of LXRs (46) and may play a significant role in mediating efflux of cholesterol to HDL receptors (45). Consistent with these findings, activation of PPARγ enhanced HDL-dependent cholesterol efflux in LXR DKO macrophages. It will be of interest to test the possibility that the induction of ABCG1 and inhibition of cholesterol esterification are mechanistically linked and represent components of a coordinated pathway for the regulation of macrophage cholesterol homeostasis. Together, these 2 PPARγ-sensitive targets provide a plausible mechanism for LXR-independent effects on macrophage foam-cell formation.

Differential roles of PPARα, β/δ, and γ agonists in regulation of macrophage lipid metabolism. In concert, the present studies define distinct biological roles of PPARα, PPARβ/δ, and PPARγ in the vascular wall. Table 2 summarizes the overlapping and receptor-specific effects of the 3 PPAR-selective agonists on metabolic parameters, atherosclerosis, and foam-cell formation. Inhibition of the expression of markers of inflammation in the artery wall was an activity shared by all 3 classes of agonists. In contrast, each agonist had a distinct effect on lipid and glucose metabolism and development of atherosclerosis. The distinct effects of each receptor-specific agonist at the whole-animal level result in part from differences in patterns of expression of their cognate receptors. However, even within the same cell type, exemplified by the macrophage foam-cell, each receptor also regulates distinct programs of gene expression. The mechanistic basis for these differential effects is unclear, but could reflect differences in target-gene recognition and/or the receptor-specific utilization of different coactivator complexes. In either case, the present studies raise the possibility that receptor-specific programs regulated by PPARα and PPARγ might be exploited therapeutically through the use of combined agonists to synergistically inhibit the development of atherosclerosis.

Methods

Animals and diet. Tenth-generation male wild-type mice (LDLR−/−/C57BL6/J, LacZ/C57BL6/J), PPARα−/−/129S4/SvJae mice, PPARα+/+/129S1/SvImJ mice (The Jackson Laboratories), and LXRα−/−/β−/− (LXR DKO) mice in a C57BL6/129S background (a gift from David Mangelsdorf, University of Texas Southwestern Medical Center, Dallas, Texas, USA) were used, beginning at 8–10 weeks of age. For the intervention study, male LDR−/− mice were matched according to initial weight and plasma cholesterol levels and fed an HC diet containing 1.25% added cholesterol and 21% milkfat (TD96121; Harlan-Teklad) for 14 weeks. Drugs were dissolved in DMSO and ether and mixed in a powder diet to provide an estimated 2.5 mg/kg/d of the PPARα agonist (GW7647, GlaxoSmithKline) (37) and 5 mg/kg/d of the PPARβ agonist (GW0742, GlaxoSmithKline) (38). An equivalent amount of solvent was mixed into the powdered diet for control animals. All animals had ad libitum access to water. Mice were weighed every 4 weeks and drug intake was adjusted according to the mean weight. Blood was obtained from animals that had fasted for 8 hours for cholesterol, triglyceride, insulin, and lipoprotein analysis, as previously described (33). Particle size distribution of the lipoproteins was determined by FPLC, using pooled samples of plasma obtained at the time of sacrifice.

For studies of gene expression in lesions, male LDR−/− mice were fed the HC diet for 3 months. After the initial induction of hypercholesterolemia, animals were grouped according to their weights and total cholesterol levels and subsequently placed on the HC diet containing either the solvent only (control), GW7647 (2.5 mg/kg/d), GW0742 (5.0 mg/kg/d), or the PPARγ ligand rosiglitazone (10 mg/kg/d) for an additional 4 weeks. The animals were sacrificed, the aortic arch was isolated, and total RNA was extracted. All animal experiments were approved by the University of California, San Diego Animal Subjects Committee.

Atherosclerosis. Atherosclerosis was quantified by computer-assisted image analysis in Sudan-stained en face preparations of the entire aorta (62) and in cross-sections through the aortic origin, as previously described (33, 63).

Preparation of lipoproteins. LDL and HDL were prepared from healthy human volunteers by ultracentrifugation (64). We prepared oxLDL and ^{125}I-labeled oxLDL as previously described (65). We generated acLDL using sodium acetate and acetic anhydride (66), and agLDL was made by vigorously vortexing the LDL for 3 minutes.

Isolation of peritoneal macrophages and treatment with agonists, in vitro. Peritoneal macrophages were isolated 4 days after intraperitoneal injection of 3 ml of thioglycollate (Sigma-Aldrich). Five million peritoneal cells were plated onto 60-mm plates in 10% FBS (Gemini Bio-Products) in RPMI 1640 medium (Cellgro, Mediatech Inc.) and allowed to adhere for 4 hours. Cholesterol and triglycerides were then extracted in hexane/isopropanol (3:2) (67, 68). Free cholesterol and total cholesterol were determined by gas chromatography (Hewlett Packard). We used 10 μg of stigmasterol (Sigma-Aldrich) as the internal standard. Cholesterol ester was estimated by subtracting free cholesterol from total cholesterol. Triglyceride content was measured by colorimetric assay (Sigma-Aldrich). Additionally, macrophages were plated onto glass microscope slides, fixed with 5% paraformaldehyde for 15 minutes, and stained with Oil red O and hematoxylin (69). For some studies, macrophages were obtained from mice fed the HC diet and plated at a density of 5 million cells/well in 6-well plates in 10% FBS in RPMI, changing the medium every 2 days. On day 4, cells were incubated with the following ligands: GW7647, 100 nM/ml; GW0742, 1.0 μM/ml; and rosiglitazone, 10 μM/ml in 1% delipidated, charcoal-stripped FBS in RPMI. Cells were harvested for RNA analysis 24 hours later.

RNA isolation from aortas, monocytes, and macrophages. For the isolation of total RNA, aortas were perfused with ice-cold PBS-EDTA followed by a 10% glacial acetic acid/EtOH solution, as described (33). Six aortic arches were pooled per group to give equivalent weights, and then homogenized. For macrophages,

Table 3
Primers and probes used for real-time PCR

Gene	Accession #	Forward primer	Reverse primer	Probe
PPARα	NM_011144	5′-GGACCTTCGGCAGCTGGT-3′	5′-TCGGACTCGGTCTTCTTGATG-3′	5′-CGGAGCATGCGCAGCTCGTACA-3′
PPARβ	XM_128500	5′-CGGAGCATGCGCAGCTCGTACA-3′	5′-CCGGTCTCCACACAGAATGAT-3′	5′-ACCTGGCGCTCTTCATCGCGG-3′
PPARγ	NM_011146	5′-CATTCTGGCCCACCAACTTC-3′	5′-TCAAAGGAATGCGAGTGGTCTT-3′	5′-TCAGCTCTGTGGACCTCTCCGTGATG-3′
LXRα	AF085745	5′-CCTTCCTCAAGGACTTCAGTTACAA-3′	5′-CATGGCTCTGGAGAACTCAAAGAT-3′	5′-AAGACTTTG CCAAAGCAGGGCTGCA-3′
LXRβ	NM_009473	5′-AAGGACTTCACCTACAGCAAGGA-3′	5′ GAACTCGAAGATGGGATTGATGA-3′	5′-ACTTCCACCGTGCAGGCTTGCAGG-3′
ABCA1	NM_013454	5′-GCGGACCTCCTGGGTGTT-3′	5′-CAAGAATCTCCGGGCTTTAGG-3′	5′-TGGATGAACCAACCACAGGCATGG-3′
ABCG1	NM_009593	5′-AAGGCCTACTACCTGGCAAAGA-3′	5′-GCAGTAGGCCACAGGGAACA-3′	5′-CATGGCCGATGTCCCCTTTCAGATC-3′
ACAT1	NM_009230	5′-GTTTGAAGTGGACCACATCAGAAC-3′	5′-CGATCGTGCTGAGGACGAA-3′	5′-TTACCACATGTTCATCGCACTCCTCATCCT-3′
IL-1β	NM_008361	5′-AGGCAGGCAGTATCACTCATTGT-3′	5′-GGAAGGTCCACGGGAAAGA-3′	5′-TGTGGGAGAAGCTGTGGCAGCTACCTGT-3′
IFN-γ	K00083	5′-CAATGAACGCTACACACTGCATCT-3′	5′-CGTGGCAGTAACAGCCAGAA-3′	5′-TGGCTTTGCAGCTCTTCCTCATGGC-3′
ICAM-1	NM_010493	5′-CGCAAGTCCAATTCACACTGA-3′	5′-CCAGAGCGGCAGAGCAA-3′	5′-TGCCAGCTCGGAGGATCACAAACG-3′

total RNA was isolated from 5 million adherent cells. The RNA was isolated using RNeasy columns and then treated with DNase (QIAGEN).

Real-time PCR–based quantitative gene expression analysis. Real-time PCR analysis was performed using the PerkinElmer ABI Prism 7700 and Sequence Detection System software (PerkinElmer Life Sciences). We used 2–5 μg of total RNA for reverse transcription using oligo-dT$_{(T12-18)}$ and the First Strand Synthesis Kit (Invitrogen Corp.). For a negative control, Superscript II was omitted from the RNA sample. Primers and probes for *CD36*, *macrosialin*, *MCP-1*, *TNF-α*, *VCAM-1*, and *GAPDH* were previously described (33). Additional primers and probes used for these studies are listed in Table 3. All samples were run in triplicate.

Western blot analysis for ABCA1. Western blot analysis was performed using 10^7 thioglycollate-elicited macrophages, as previously described (70). Unboiled cell lysate (25 μg) was loaded onto a 3–8% Tris-Acetate NuPAGE gel (Invitrogen Corp.). After determining the efficiency of protein transfer and well-to-well variability with Ponceau Red (Sigma-Aldrich), the nitrocellulose membrane (Invitrogen Corp.) was incubated with an ABCA1 polyclonal antibody (Novus Biological) at a dilution of 1:1,000 in 5% milk/PBS with 0.1% Tween (polyoxyethylene sorbitan monolaurate; Fisher Chemicals) overnight at 4°C. The next day, the membrane was washed in PBS with 0.1% Tween before adding anti-rabbit IgG-HRP at dilutions of 1:5,000 (Dako) in 5% milk/PBS with 0.1% Tween and then incubated for 1 hour at room temperature. Bands were visualized using the Supersignal West Pico Chemical Luminescence Substrate (Pierce Biotechnology Inc.). Western blot analysis for β-actin was performed to correct for well-to-well variability.

Oxidized LDL binding and degradation assays. Uptake and degradation of oxLDL was measured as described (71) with minor modifications. Thioglycollate-elicited peritoneal macrophages were plated at a density of 5×10^5 cells/well in 24-well plates, and the medium was changed every 2 days. On day 4, triplicate wells were treated with PPAR agonists in 1% delipidated and charcoal-stripped FBS in RPMI for 24 hours. The cells were washed with PBS and then incubated with ^{125}I-oxLDL at a concentration of 5 μg/ml in 1% delipidated and charcoal-stripped FBS in RPMI. For ligand association assays, cells were incubated for 5 hours at 37°C. Cells were placed on ice for 15 minutes and then washed in ice-cold 1% BSA-PBS and PBS and then lysed in 500 μl of NaOH (0.2 N). We assayed 100-μl aliquots for ^{125}I radioactivity and protein concentration. For degradation measurements, the medium was subjected to tricholoracetic acid precipitation, and 100 μl of the tricholoracetic acid–soluble solution was assayed for ^{125}I radioactivity. Specific binding and degradation was calculated by subtracting nonspecific binding and degradation determined in the presence of a 20-fold excess of unlabeled oxLDL. Protein concentration was determined by the Bradford method (72). Results were also corrected for degradation in the absence of cells.

Cholesterol efflux assays. Cholesterol efflux assays were performed as described (73) with minor modifications. Thioglycollate-elicited peritoneal macrophages were plated at a density of 1×10^6 cells/well in 24-well plates. After 4 days, triplicate wells were washed in PBS and treated with PPAR agonist at concentrations previously stated or with the LXR agonist 24 (S), -25-epoxycholesterol (2 μM/ml) for 24 hours in 1% delipidated and charcoal-stripped FBS in RPMI. After 48 hours, cells were loaded with 2 μCi/ml of ^{3}H cholesterol (Perkin Elmer Life Sciences) and 50 μg/ml of acLDL in the presence of PPAR or LXR agonists for another 48 hours. After loading, the cells were again washed in PBS, and then fresh medium with ligands was added. After 4 hours of equilibration, the medium was replaced with fresh medium containing human apoAI (20 μg/ml) (Intracel Corp.) or human HDL (100 μg/ml) plus agonists. The cells were incubated overnight at 37°C, and then 200 μl of medium was removed and filtered (MultiScreen-HV plates, Millipore Corp.) to remove any cell debris and ^{3}H radioactivity was determined. Adherent cells were washed with PBS and then lysed in 500 μl of 0.2 N NaOH. We used 100-μl aliquots for determination of ^{3}H radioactivity and protein content. Results are expressed as the percentage of ^{3}H cholesterol in the medium divided by the total ^{3}H cholesterol in the medium and cells per milligram of protein.

Cholesterol esterification assays. Cholesterol esterification was measured as described (43) with the following modifications. Thioglyocollate-elicited peritoneal macrophages were isolated from LXR wild-type and LXR DKO mice and plated into 24-well plates at a density of 10^6 cells/well. After 2 days of treatment with PPAR agonists and an ACAT inhibitor (GW4517, a gift from Nigel Ramsden, Glaxo Wellcome Research), agLDL (100 μg/ml) was added to the media and the cells were incubated for 3 hours. Cells were briefly rinsed in PBS, resuspended in medium plus drug, and incubated with 5 μl of an ethanol mixture containing 0.5 μCi of C^{14} oleic acid (GE Lifesciences) and a 25 M excess of cold oleic acid for 4 hours. Cells were washed twice in ice-cold PBS containing 0.1% BSA, then 3 times with ice-cold PBS, and lipids were extracted, dried under nitrogen, and resuspended in 200 μl chloroform. The lipid suspension (100 μl) was spotted and separated by TLC using a hexane/ethyl ether/glacial acetic acid (80:20:1) solvent. After exposing the TLC plates to x-ray film, spots representing the cholesteryl ester and free oleic acid were cut out and counted. Results are expressed as the percentage of labeled oleic acid incorporated into cholesterol ester.

Transfer of peritoneal macrophages from PPARα$^{-/-}$ and LXR DKO mice into LDLR$^{-/-}$ mice. Male donor mice were injected intraperitoneally with thioglycollate. After 4 days, the animals were sacrificed and their peritoneal cells were isolated, red blood cells were lysed, and the remaining cells were counted. Thirty million cells were then injected intraperitoneally into recipient hypercholesterolemic LDLR$^{-/-}$ male mice fed either the

control or HC diet and treated with specific PPAR agonists as indicated. Three days later, the recipient mice were sacrificed and their peritoneal macrophages were isolated for lipid staining and quantification of cholesterol and triglyceride contents.

Bone marrow reconstitution studies. Bone marrow progenitor cells were isolated by flushing the femurs and tibias from LXR DKO male mice (8–12 weeks of age) with ice-cold PBS. Red blood cells were lysed and the bone marrow progenitor cells were washed and concentrated in PBS. We retro-orbitally injected 2×10^6 cells (suspended in 100 μl PBS) into 6–8 week old LDLR$^{-/-}$ male mice that received 1,000 rad 3 hours prior to injection. After 4 weeks on the standard chow diet, the bone marrow–reconstituted animals were placed on the 1.25% cholesterol and 21% milkfat diet plus either the PPARα or γ selective agonist for 16 weeks. They were then injected with thioglycollate (intraperitoneally) and their peritoneal macrophages were isolated. The macrophages were either stained with Oil red O, or their total RNA was isolated and reverse-transcribed for real-time PCR analysis as previously described.

Statistical analysis. Groups were compared by unpaired *t* tests or one-way ANOVA analysis and ad hoc Tukey-Kramer multiple comparisons using InStat software (Graphpad Software). *P* values less than or equal to 0.05 are considered significant.

Acknowledgments

Address correspondence to: Andrew C. Li, Department of Cellular and Molecular Medicine, Medical Teaching Facility, Room 109, University of California, San Diego, 9500 Gilman Drive, La Jolla, California 92093-0682, USA. Phone: (858) 534-0575; Fax: (858) 822-2127; E-mail: acli@ucsd.edu. Or to: Christopher K. Glass, Department of Cellular and Molecular Medicine and Department of Medicine, Room 217, University of California, San Diego, 9500 Gilman Drive, La Jolla, California 92093-0651, USA. Phone: (858) 534-0611; Fax: (858) 822-2127; E-mail: cglass@ucsd.edu.

The Glass and Palinski laboratories contributed equally to this work.

1. Issemann, I., Prince, R.A., Tugwood, J.D., and Green, S. 1993. The peroxisome proliferator-activated receptor: retinoid X receptor heterodimer is activated by fatty acids and fibrate hypolipidaemic drugs. *J. Mol. Endocrinol.* **11**:37–47.
2. Willson, T., Brown, P., Sternbach, D., and Henke, B. 2000. The PPARs: From orphan receptors to drug discovery. *J. Med. Chem.* **43**:527–550.
3. Chawla, A., Repa, J., Evans, R., and Mangelsdorf, D. 2001. Nuclear receptors and lipid physiology: Opening the X-files. *Science.* **294**:1866–1870.
4. Barbier, O., et al. 2002. Pleiotropic actions of peroxisome proliferator-activated receptors in lipid metabolism and atherosclerosis. *Arterioscler. Thromb. Vasc. Biol.* **22**:717–726.
5. Bardot, O., Aldridge, T.C., Latruffe, N., and Green, S. 1993. PPAR-RXR heterodimer activates a peroxisome proliferator response element upstream of the bifunctional enzyme gene. *Biochem. Biophys. Res. Commun.* **192**:37–45.
6. Jiang, C., Ting, A.T., and Seed, B. 1998. PPAR-gamma agonists inhibit production of monocyte inflammatory cytokines. *Nature.* **391**:82–86.
7. Marx, N., Schönbeck, U., Lazar, M.A., Libby, P., and Plutzky, J. 1998. Peroxisome proliferator-activated receptor gamma activators inhibit gene expression and migration in human vascular smooth muscle cells. *Circ. Res.* **83**:1097–1103.
8. Staels, B., et al. 1998. Activation of human aortic smooth-muscle cells is inhibited by PPARalpha but not by PPARgamma activators. *Nature.* **393**:790–793.
9. Ricote, M., Li, A.C., Willson, T.M., Kelly, C.J., and Glass, C.K. 1998. The peroxisome proliferator-activated receptor-γ is a negative regulator of macrophage activation. *Nature.* **391**:79–82.
10. Delerive, P., et al. 1999. Peroxisome proliferator-activated receptor alpha negatively regulates the vascular inflammatory gene response by negative cross-talk with transcription factors NF-kappaB and AP-1. *J. Biol. Chem.* **274**:32048–32054.
11. Ricote, M., et al. 1998. Expression of the peroxisome proliferator-activated receptor γ (PPARγ) in human atherosclerosis and regulation in macrophages by colony stimulating factors and oxidized low density lipoprotein. *Proc. Natl. Acad. Sci. U. S. A.* **95**:7614–7619.
12. Marx, N., Sukhova, G., Murphy, C., Libby, P., and Plutzky, J. 1998. Macrophages in human atheroma contain PPARgamma: differentiation-dependent peroxisomal proliferator-activated receptor gamma (PPARgamma) expression and reduction of MMP-9 activity through PPARgamma activation in mononuclear phagocytes in vitro. *Am. J. Pathol.* **153**:17–23.
13. Law, R.E. 2000. Expression and function of PPARgamma in rat and human vascular smooth muscle cells. *Circulation.* **101**:1311–1318.
14. Sueyoshi, S., et al. 2001. Expression of peroxisome proliferator-activated receptor subtypes in human atherosclerosis. *Ann. N. Y. Acad. Sci.* **947**:429–432.
15. Clark, R.B., et al. 2000. The nuclear receptor PPAR gamma and immunoregulation: PPAR gamma mediates inhibition of helper T cell responses. *J. Immunol.* **164**:1364–1371.
16. Lee, H., et al. 2000. Role for peroxisome proliferator-activated receptor alpha in oxidized phospholipid-induced synthesis of monocyte chemotactic protein-1 and interleukin-8 by endothelial cells. *Circ. Res.* **87**:516–521.
17. Gosling, J., et al. 1999. MCP-1 deficiency reduces susceptibility to atherosclerosis in mice that overexpress human apolipoprotein B. *J. Clin. Invest.* **103**:773–778.
18. Boring, L., Gosling, J., Cleary, M., and Charo, I.F. 1998. Decreased lesion formation in CCR2–/– mice reveals a role for chemokines in the initiation of atherosclerosis. *Nature.* **394**:894–897.
19. Gu, L., et al. 1998. Absence of monocyte chemoattractant protein-1 reduces atherosclerosis in low density lipoprotein receptor-deficient mice. *Mol. Cell.* **2**:275–281.
20. Tontonoz, P., Nagy, L., Alvarez, J.G.A., Thomazy, V.A., and Evans, R.M. 1998. PPARγ promotes monocyte/macrophage differentiation and uptake of oxidized LDL. *Cell.* **93**:241–252.
21. Febraio, M., et al. 2000. Targeted disruption of the class B scavenger receptor CD36 protects against atherosclerotic lesion development in mice. *J. Clin. Invest.* **105**:1049–1056.
22. Jackson, S.M., et al. 1999. Peroxisome proliferator-activated receptor activators target human endothelial cells to inhibit leukocyte-endothelial cell interaction. *Arterioscler. Thromb. Vasc. Biol.* **19**:2094–2104.
23. Pasceri, V., Wu, H.D., Willerson, J.T., and Yeh, E.T. 2000. Modulation of vascular inflammation in vitro and in vivo by peroxisome proliferator-activated receptor-gamma activators. *Circulation.* **101**:235–238.
24. Han, K., et al. 2000. Oxidized LDL reduces monocyte CCR2 expression through pathways involving peroxisome proliferator-activated receptor γ. *J. Clin. Invest.* **106**:793–802.
25. Marx, N., et al. 2002. PPAR activators as antiinflammatory mediators in human T lymphocytes: implications for atherosclerosis and transplantation-associated arteriosclerosis. *Circ. Res.* **90**:703–710.
26. Chawla, A., et al. 2001. A PPAR gamma-LXR-ABCA1 pathway in macrophages is involved in cholesterol efflux and atherogenesis. *Mol. Cell.* **7**:161–171.
27. Chinetti, G., et al. 2001. PPAR-alpha and PPAR-gamma activators induce cholesterol removal from human macrophage foam cells through stimulation of the ABCA1 pathway. *Nat. Med.* **7**:53–58.
28. Oliver, W.R., Jr., et al. 2001. A selective peroxisome proliferator-activated receptor delta agonist promotes reverse cholesterol transport. *Proc. Natl. Acad. Sci. U. S. A.* **98**:5306–5311.
29. Vosper, H., et al. 2001. The peroxisome proliferator-activated receptor delta promotes lipid accumulation in human macrophages. *J. Biol. Chem.* **276**:44258–44265.
30. Tordjman, K., et al. 2001. PPARα deficiency reduces insulin resistance and atherosclerosis in apoE-null mice. *J. Clin. Invest.* **107**:1025–1034.
31. Claudel, T., et al. 2001. Reduction of atherosclerosis in apolipoprotein E knockout mice by activation of the retinoid X receptor. *Proc. Natl. Acad. Sci. U. S. A.* **98**:2610–2615.
32. Duez, H., et al. 2002. Reduction of atherosclerosis by the peroxisome proliferator-activated receptor alpha agonist fenofibrate in mice. *J. Biol. Chem.* **277**:48051–48057.
33. Li, A., et al. 2000. Peroxisome proliferator–acti-

vated receptor γ ligands inhibit development of atherosclerosis in LDL receptor–deficient mice. *J. Clin. Invest.* **106**:523–531.

34. Collins, A.R., et al. 2001. Troglitazone inhibits formation of early atherosclerotic lesions in diabetic and nondiabetic low density lipoprotein receptor-deficient mice. *Arterioscler. Thromb. Vasc. Biol.* **21**:365–371.

35. Chen, Z., et al. 2001. Troglitazone inhibits atherosclerosis in apolipoprotein E-knockout mice: pleiotropic effects on CD36 expression and HDL. *Arterioscler. Thromb. Vasc. Biol.* **21**:372–377.

36. Lee, C.H., et al. 2003. Transcriptional repression of atherogenic inflammation: modulation by PPARdelta. *Science*. **302**:453–457.

37. Brown, P.J., et al. 2001. Identification of a subtype selective human PPARalpha agonist through parallel-array synthesis. *Bioorg. Med. Chem. Lett.* **11**:1225–1227.

38. Sznaidman, M.L., et al. 2003. Novel selective small molecule agonists for peroxisome proliferator-activated receptor delta (PPARdelta)-synthesis and biological activity. *Bioorg. Med. Chem. Lett.* **13**:1517–1521.

39. Chawla, A., et al. 2001. PPAR-gamma dependent and independent effects on macrophage-gene expression in lipid metabolism and inflammation. *Nat. Med.* **7**:48–52.

40. Gossen, J.A., et al. 1989. Efficient rescue of integrated shuttle vectors from transgenic mice: a model for studying mutations in vivo. *Proc. Natl. Acad. Sci. U. S. A.* **86**:7971–7975.

41. Schultz, J.R., et al. 2000. Role of LXRs in control of lipogenesis. *Genes Dev.* **14**:2831–2838.

42. Chinetti, G., et al. 1998. Activation of proliferator-activated receptors α and γ induces apoptosis of human monocyte-derived macrophages. *J. Biol. Chem.* **273**:25573–25580.

43. Tabas, I., Boykow, G.C., and Tall, A.R. 1987. Foam cell-forming J774 macrophages have markedly elevated acyl coenzyme A:cholesterol acyl transferase activity compared with mouse peritoneal macrophages in the presence of low density lipoprotein (LDL) despite similar LDL receptor activity. *J. Clin. Invest.* **79**:418–426.

44. Wang, N., Lan, D., Chen, W., Matsuura, F., and Tall, A.R. 2004. ATP-binding cassette transporters G1 and G4 mediate cellular cholesterol efflux to high-density lipoproteins. *Proc. Natl. Acad. Sci. U. S. A.* **101**:9774–9779.

45. Klucken, J., et al. 2000. ABCG1 (ABC8), the human homolog of the Drosophila white gene, is a regulator of macrophage cholesterol and phospholipid transport. *Proc. Natl. Acad. Sci. U. S. A.* **97**:817–822.

46. Venkateswaran, A., et al. 2000. Human white/murine

ABC8 mRNA levels are highly induced in lipid-loaded macrophages. A transcriptional role for specific oxysterols. *J. Biol. Chem.* **275**:14700–14707.

47. Ye, J.M., et al. 2001. Peroxisome proliferator-activated receptor (PPAR)-alpha activation lowers muscle lipids and improves insulin sensitivity in high fat-fed rats: comparison with PPAR-gamma activation. *Diabetes*. **50**:411–417.

48. Vu-Dac, N., et al. 1998. The nuclear receptors peroxisome proliferator-activated receptor alpha and Rev-erbalpha mediate the species-specific regulation of apolipoprotein A-I expression by fibrates. *J. Biol. Chem.* **273**:25713–25720.

49. Glass, C., and Witztum, J. 2001. Atherosclerosis; the road ahead. *Cell*. **104**:503–516.

50. Li, A.C., and Glass, C.K. 2002. The macrophage foam cell as a target for therapeutic intervention. *Nat. Med.* **8**:1235–1242.

51. Libby, P., Ridker, P.M., and Maseri, A. 2002. Inflammation and atherosclerosis. *Circulation*. **105**:1135–1143.

52. Dansky, H.M., Charlton, S.A., Harper, M.M., and Smith, J.D. 1997. T and B lymphocytes play a minor role in atherosclerotic plaque formation in the apolipoprotein E-deficient mouse. *Proc. Natl. Acad. Sci. U. S. A.* **94**:4642–4646.

53. Song, L., Leung, C., and Schindler, C. 2001. Lymphocytes are important in early atherosclerosis. *J. Clin. Invest.* **108**:251–259. doi:10.1172/JCI200111380.

54. Tangirala, R.K., et al. 2002. Identification of macrophage liver X receptors as inhibitors of atherosclerosis. *Proc. Natl. Acad. Sci. U. S. A.* **99**:11896–11901.

55. Joseph, S.B., et al. 2002. Synthetic LXR ligand inhibits the development of atherosclerosis in mice. *Proc. Natl. Acad. Sci. U. S. A.* **99**:7604–7609.

56. Galetto, R., Albajar, M., Polanco, J.I., Zakin, M.M., and Rodriguez-Rey, J.C. 2001. Identification of a peroxisome-proliferator-activated-receptor response element in the apolipoprotein E gene control region. *Biochem. J.* **357**:521–527.

57. Chinetti, G., Lestavel, S., Fruchart, J.C., Clavey, V., and Staels, B. 2003. Peroxisome proliferator-activated receptor alpha reduces cholesterol esterification in macrophages. *Circ. Res.* **92**:212–217.

58. Yagu, H., et al. 2000. Absence of ACAT-1 attenuates atherosclerosis but causes dry eye and cutaneous xanthomatosis in mice with congenital hyperlipidemia. *J. Biol. Chem.* **275**:21324–21330.

59. Fazio, S., et al. 2001. Increased atherosclerosis in LDL receptor–null mice lacking ACAT1 in macrophages. *J. Clin. Invest.* **107**:163–171.

60. Kusunoki, J., et al. 2001. Acyl-CoA:cholesterol acyltransferase inhibition reduces atherosclerosis in apolipoprotein E-deficient mice. *Circulation*. **103**:2604–2609.

61. Welch, J.S., Ricote, M., Akiyama, T.E., Gonzalez, F.J.,

and Glass, C.K. 2003. PPARgamma and PPARdelta negatively regulate specific subsets of lipopolysaccharide and IFN-gamma target genes in macrophages. *Proc. Natl. Acad. Sci. U. S. A.* **100**:6712–6717.

62. Palinski, W., et al. 1994. Apoprotein E-deficient mice are a model of lipoprotein oxidation in atherogenesis: Demonstration of oxidation-specific epitopes in lesions and high titers of autoantibodies to malondialdehyde-lysine in serum. *Arterioscler. Thromb.* **14**:605–616.

63. Paigen, B., Morrow, A., Holmes, P.A., Mitchell, D., and Williams, R.A. 1987. Quantitative assessment of atherosclerotic lesions in mice. *Atherosclerosis*. **68**:231–240.

64. Havel, R.J., Eder, H.A., and Bragdon, J.H. 1955. The distribution and chemical composition of ultracentrifugally separated lipoproteins in human serum. *J. Clin. Invest.* **34**:1345–1353.

65. Boullier, A., et al. 2000. The binding of oxidized low density lipoprotein to mouse CD36 is mediated in part by oxidized phospholipids that are associated with both the lipid and protein moieties of the lipoprotein. *J. Biol. Chem.* **275**:9163–9169.

66. Goldstein, J.L., Ho, Y.K., Basu, S.K., and Brown, M.S. 1979. Binding site on macrophages that mediates uptake and degradation of acetylated low density lipoprotein, producing massive cholesterol deposition. *Proc. Natl. Acad. Sci. U. S. A.* **76**:333–337.

67. Moore, G.L., and Davis, R.A. 2002. Expression of cholesterol-7alpha-hydroxylase in murine macrophages prevents cholesterol loading by acetyl-LDL. *J. Lipid Res.* **43**:629–635.

68. Miyake, J.H., et al. 2002. Transgenic expression of cholesterol-7-alpha-hydroxylase prevents atherosclerosis in C57BL/6J mice. *Arterioscler. Thromb. Vasc. Biol.* **22**:121–126.

69. Sheehan, D.C., and Hrapchak, B.B. 1980. *Theory and practice of histotechnology*. C.V. Mosby Co. St. Louis, Missouri, USA. 481 pp.

70. Welch, J.S., et al. 2002. TH2 cytokines and allergic challenge induce Ym1 expression in macrophages by a STAT6-dependent mechanism. *J. Biol. Chem.* **277**:42821–42829.

71. Gillotte-Taylor, K., Boullier, A., Witztum, J.L., Steinberg, D., and Quehenberger, O. 2001. Scavenger receptor class B type I as a receptor for oxidized low density lipoprotein. *J. Lipid Res.* **42**:1474–1482.

72. Bradford, M.M. 1976. A rapid and sensitive method for the quantitation of microgram quantities of protein utilizing the principle of protein-dye binding. *Anal. Biochem.* **72**:248–254.

73. Gillotte, K.L., Davidson, W.S., Lund-Katz, S., Rothblat, G.H., and Phillips, M.C. 1998. Removal of cellular cholesterol by pre-beta-HDL involves plasma membrane microsolubilization. *J. Lipid Res.* **39**:1918–1928.